# Characteristics and degradation of organic aerosols from cooking sources based on hourly observation of organic molecular markers in urban environment

**Rui Li [a, b#], Kun Zhang [a, b#], Qing Li [a, b], Liumei Yang [a, b], Shunyao Wang [a, b], Zhiqiang Liu [a, b, c], Xiaojuan Zhang [a, b, c], Hui Chen [a, b], Yanan Yi [a, b], Jialiang Feng [a, b], Qiongqiong Wang [d], Ling Huang [a, b], Wu Wang [a, b], Yangjun Wang [a, b], Jian Zhen Yu [e, f], Li Li [a, b*]**

[a] School of Environmental and Chemical Engineering, Shanghai University, Shanghai, China

[b] Key Laboratory of Organic Compound Pollution Control Engineering (MOE), Shanghai University, Shanghai, China

[c] Jiangsu Changhuan Environment Technology Co., Ltd., Changzhou, Jiangsu, China

[d] School of Environmental Studies, China University of Geosciences, Wuhan, 430074, China

[e] Department of Chemistry, Hong Kong University of Science & Technology, Hong Kong, China

[f] Division of Environment & Sustainability, Hong Kong University of Science & Technology, Hong Kong, China

\# These two authors contributed equally to this work.

*\* Correspondence: Li Li (Lily@shu.edu.cn)*

**Abstract**

Molecular markers in organic aerosol (OA) provide specific source information of PM$_{2.5}$, and the contribution of cooking organic aerosols to OA is significant, especially in urban environments. However, the low time resolution of offline measurements limits the effectiveness in interpreting the tracer data, the diurnal variation of cooking emission and the oxidation process. In this study, we used on-line thermal desorption aerosol gas chromatography mass spectrometry (TAG) to measure organic molecular markers in fine particulate matter (PM$_{2.5}$) at an urban site in Changzhou, China. The concentrations of saturated fatty acids (sFA), unsaturated fatty acids (uFAs), and oxidative decomposition products of unsaturated fatty acids (ODPs) were measured every two hours to investigate the temporal variations and the oxidative decomposition characteristics of uFAs in urban environment. The average concentration of total fatty acids (TFAs, sum of sFAs and uFAs) was measured to be 105.70± 230.28 ng/m$^3$. The average concentration of TFAs in polluted period (PM$_{2.5}$

28    ≥ 35 μg/m$^3$) was 147.06 ng/m$^3$, which was 4.2 times higher than that in clean period (PM$_{2.5}$ < 35 μg/m$^3$), higher than the

29    enhancement of PM$_{2.5}$ (2.2 times) and organic carbon (OC) (2.0 times) concentrations comparing polluted period to clean

30    period. The mean concentration of cooking aerosol in the polluted period (4.0 μg/m$^3$) was about 5.3 times higher than that

31    in the clean period (0.75 μg/m$^3$), which was similar to the trend of fatty acids. Fatty acids showed a clear diurnal variation.

32    Linoleic acid /stearic acid and oleic acid / stearic acid ratios were significantly higher at dinner time, and closer to the

33    cooking source profile. By performing backward trajectory clustering analysis, under the influence of short-distance air

34    masses from surrounding areas, the concentrations of TFAs and PM$_{2.5}$ were relatively high; while under the influence of

35    air masses from easterly coastal areas, the oxidation degree of uFAs emitted from local culinary sources were higher. The

36    effective rate constants ($k_O$) for the oxidative degradation of oleic acid were estimated to be 0.08-0.57 h$^{-1}$, which were lower

37    than $k_L$ (the estimated effective rate constants of linoleic acid, 0.16-0.80 h$^{-1}$). Both $k_O$ and $k_L$ showed a significant positive

38    correlation with O$_3$, indicating that O$_3$ was the main night-time oxidants for uFAs in the Changzhou City. Using fatty acids

39    as tracers, cooking was estimated to contribute an average of 4.6% to PM$_{2.5}$ concentrations, increased to 7.8% at 20:00.

40    Cooking was an important source to OC, contributing to 8.1%, higher than the contribution to PM$_{2.5}$. This study investigates

41    the variation of the concentrations and oxidative degradation of fatty acids and corresponding oxidation products in ambient

42    air, which can be a guide for the refinement of aerosol source apportionment, and provide scientific support for the

43    development of cooking source control policies.

44    **1. Introduction**

45    Organic aerosol (OA) is an important component of fine particulate matter (PM$_{2.5}$), accounting for 20-90% of the total

46    PM$_{2.5}$ mass (Kanakidou et al., 2005). Among different OA sources, restaurant fumes are relatively important (Huang et al.,

47    2021). The contribution of cooking organic aerosols (COA) to OA is significant, especially in urban environments, where

48    COA can contribute 11%-34% to total organic carbon (OC) and 3%-9% to PM$_{2.5}$ mass concentration, even higher than

49    traffic-related hydrocarbon-based OA (Huang et al., 2021; Li et al., 2020). The presence of carcinogenic mutagens in

50    restaurant fumes contains chemicals that can be harmful to human immune function (Huang et al., 2020). According to the

51    2018 global cancer statistics, lung cancer accounts for 24.1% of all cancer deaths in China and is the most common cause

52    of cancer-related deaths in China. The carcinogenic risk analysis suggested that the potentially adverse health effects

53    induced by cooking sources should not be ignored (Zhang et al., 2017a).

54    Cooking is an important source contributor to PM$_{2.5}$, especially in urban environments. Cooking sources have recently

55    received increasing attention, but they are largely an uncontrolled source of PM$_{2.5}$. Saturated fatty acids (sFAs) and

unsaturated fatty acids (uFAs), such as palmitic, stearic, and oleic acids, are known molecular markers from cooking emissions, which are released primarily during cooking activities from the hydrolysis and thermal oxidation of cooking oils. Fatty acids and their derivatives are often used as tracers in the receptor model for the source apportionment of $PM_{2.5}$. It has been found that nonanoic acid, 9-oxononanoic acid and azelaic acid are the main atmospheric oxidation products of oleic acid in the aerosol, while uFAs such as oleic and linoleic acids also react with other atmospheric oxidants, such as hydroxyl (OH) (Nah et al., 2014; Wang et al., 2020).

In previous studies on the molecular tracers of cooking source based on filter membrane sampling, the time resolution usually varies from one day to several days, which cannot accurately capture the diurnal variations of pollutants emitted by the cooking source (Li et al., 2021). The thermal desorption aerosol gas chromatography−mass spectrometry (TAG) enables online monitoring of organic molecular markers (Wang et al., 2020). By clarifying the characteristics of cooking emissions, quantifying the concentrations of pollutants emitted from cooking and its contribution to urban OA on the diurnal time scales, we build up data and process knowledge about cooking-source $PM_{2.5}$ pollution, which in turn help us to evaluate the option of controlling cooking emissions in the overall pollution prevention for urban environments.

Processes such as emission rate, atmospheric dilution, and photochemical oxidation can affect aerosol composition measured at receptor sites (Fortenberry et al., 2019; Yee et al., 2018). Particulate organic matter can undergo heterogeneous oxidation by ozone, OH and nitrate ($NO_3$) radicals (Wang et al., 2020). When using organic tracer data from filter analysis, variations in concentration due to degradation or secondary production were reported (Ringuet et al., 2012). These degradation and generation processes in the atmosphere are therefore worthy of our attention when using organic markers as source tracers. The mechanism and kinetics of ozonolysis of oleic acid and linoleic acid in the presence of oxidants such as $NO_3$, $O_3$ and OH radicals have been extensively studied in the laboratory studies (Vesna et al., 2009; Zahardis and Petrucci, 2007; Ziemann, 2005). The aging of POA markers under atmospheric conditions, however, is still far from being properly understood with few field observations performed in this topic compared to laboratory studies (Bertrand et al., 2018a; Bertrand et al., 2018b). The high timely-resolved observations would help to fill this gap.

In this study, TAG was employed at an urban site in Changzhou, China, to investigate the variation of atmospheric cooking-related fatty acids with hourly resolution data (Ren et al., 2019). The aim of this study is to identify the contribution of cooking emissions to ambient $PM_{2.5}$ with hourly organic molecular data and to investigate the oxidative decomposition reactions of cooking-related uFAs in an urban area. Results of this study could provide valid basis and insights for the refinement of $PM_{2.5}$ source apportionment as well as atmospheric modelling.

## 2. Methodology

### 2.1 Field measurement

Gaseous pollutants, PM$_{2.5}$ and its main chemical constituents (water soluble ions, carbon components and elements, etc.) as well as organic markers (alkanes, hopanes, polycyclic aromatic hydrocarbons, sugars, alcohols and organic acids, etc.) were measured online at the Changzhou Environmental Monitoring Center of Jiangsu Province (CEMC) (31.76N, 119.96E) during January-March 2021, which is a representative urban site (Fig. 1). The meteorological parameters were obtained from a meteorological monitor (WXT520, VAISALA Inc., FL). O$_3$ and NO$_2$ were measured by ozone analyzer (49i-PS, Thermo Fisher Scientific, US) and NOx analyzer (MODEL450i, Thermo Fisher Scientific, US), respectively. PM$_{2.5}$ mass concentration was measured by an online particulate matter monitor (BAM1020. Met One Inc., US); the concentration of the carbon components (Organic carbon, OC; Elemental carbon, EC) was measured using semi-continuous OC/EC analyzer (RT-4, Sunset Laboratory Inc, US) (Nicolosi et al., 2018; Zhang et al., 2017b); water soluble ions were measured by MARGA ionic online analyzer (ADI2080, Metrohm, CHN) (Makkonen et al., 2012) and elements were measured by an atmospheric elements online monitor (EHM-X200, Tianrui, CHN) (Makkonen et al., 2012).
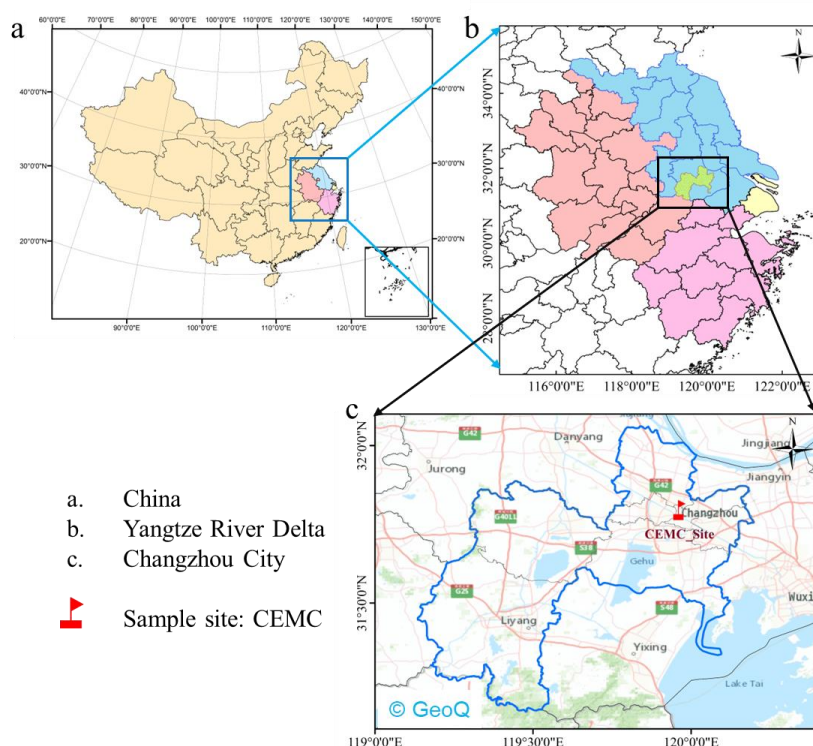
**Figure 1. Location of the sampling site in Changzhou, China.**

Quantification of hourly speciated organic markers was achieved using TAG. The operation details and data quality have been described in our previous work (Wang et al., 2020; Zhang et al., 2021). The sampling and analysis sequence of

101    the TAG system includes four steps: (a) PM$_{2.5}$ sampling and synchronous gas chromatography-mass spectrometry (GC-

102    MS) analysis of the previous sample; (b) loading of the internal standards (IS) from the standards (STD) reservoir to a

103    thermal desorption cell; (c) derivatization and thermal desorption of analytes on the collection and thermal desorption

104    (CTD) cell and subsequent preconcentration of the analytes in focusing trap (FT); and (d) loading of analytes into the GC

105    column for GC-MS analysis. The following is a detailed description. Ambient air was sampled at a flow rate of 8.5-9.5

106    L/min through a cyclone with PM$_{2.5}$ cutting size (BGI Inc., Waltham, MA), a Nafion dryer (PERMA PURE, MD-700-24S-

107    3) to remove moisture, and then through a carbon denuder (model: ADI-DEN2) to remove volatile organics. The sampled

108    particles were collected on the CTD cell at 30°C for 60 min, followed by derivatization and thermal desorption for 8 min

109    as the temperature of the CTD cell increases to 300°C in 2 min and maintains for 6 min, during which a 10 mL/min helium

110    purge flow combined with a 40 mL/min derivatization flow with N-methyl- N-(trimethylsilyl) trifluoroacetamide (MSTFA)

111    flow through for 8 min. Subsequently, the FT was heated to 300°C in 2 min and kept at 300°C for 10 min, transferring the

112    analytes onto the GC column head (DB-5MS, size 30 m × 0.25 μm × 0.25 μm) by carrier gas. After GC separation, the

113    target organics were sent to the MS detector for quantification. The GC-MS analysis duration for each sample was 60 min

114    while collection of the next sample the CTD cell starts. With the current TAG instrumental set-up, samples were collected

115    every even hour. The post-sampling steps, including in-situ derivatization, thermal desorption, GC-MS analysis, and

116    standby step, took 2 h, thus producing 12 samples per day.

117        The summary of target organic molecular markers and IS are shown in Table 1. Identification of compounds was

118    performed by comparing retention times and mass spectra with those of authentic standards (Vesna et al., 2009; Wang et

119    al., 2020). Calibration curves were established by internal standard method. The correlation coefficients of the calibration

120    curves range from 0.88-1.00. For compounds without authentic standards and for compounds whose authentic standards

121    are not included in the current standard mixture, their identification is performed by comparing their mass spectra with the

122    National Institute of Standards and Technology (NIST) libraries. Azelaic acid was identified and quantified by using

123    authentic standards. Nonanoic acid and 9-oxononanoic acid were identified by comparison with mass spectra in the NIST

124    library and by referring to Ziemann (2005), Pleik et al. (2016) and Wang et al. (2020). Ozone oxidation of oleic acid yields

125    C$_9$ aldehydes and acids including nonanal, azelaic acid, nonanoic acid, and 9-oxononanoic acid. Since nonanal could also

126    be primary in the gas phase, it is thus not discussed in this paper. The library of the NIST was identified and quantified

127    using the alternative standards specified in Table 1.

128

129

**Table 1. Statistics of hourly concentrations of organics associated with cooking emissions measured by TAG during the campaign.**

| Compounds | Average | Stdev | Min | Max | Quantification IS |
|---|---|---|---|---|---|
| Myristic acid [a] | 0.69 | 1.33 | 0.03 | 10.14 | Palmitic acid-d$_{31}$ |
| Palmitic acid | 38.77 | 84.14 | 1.45 | 670.12 | Palmitic acid-d$_{31}$ |
| Stearic acid | 26.51 | 50.58 | 1.81 | 341.65 | Palmitic acid-d$_{31}$ |
| Oleic acid | 32.15 | 81.34 | 0.96 | 723.95 | Stearic acid-d$_{35}$ |
| Linoleic acid [b] | 7.80 | 28.32 | 0.09 | 326.50 | Stearic acid-d$_{35}$ |
| Nonanoic acid [c] | 1.19 | 1.32 | BD [d] | 7.94 | Adipic acid-d$_{10}$ |
| 9-oxononanoic acid [c] | 3.91 | 4.73 | 0.19 | 17.18 | Adipic acid-d$_{10}$ |
| Azelaic acid | 9.15 | 32.99 | BD | 309.64 | Adipic acid-d$_{10}$ |

a, Quantified using palmitic acid as the surrogate; b, Quantified using oleic acid as the surrogate; c, Quantified using azelaic acid as the surrogate; d, Below detection limit.

## 2.2 Backward trajectory analysis

Backward trajectory analysis is a useful tool in identifying the influence of air masses on the chemical composition of PM$_{2.5}$ (Wang et al., 2017). Backward trajectories of 36-h duration arriving at an altitude of 100 m above ground level (AGL) over the CEMC site were calculated deploying the 0.5° Global Data Assimilation System (GDAS) meteorological data (https://www.ready.noaa.gov/archives.php, last access: Aug 16, 2022). The trajectories were then classified into different clusters according to the geographical origins and movement of the trajectories using the TrajStat model (Li et al., 2020).

## 2.3 Relative rate constant analysis

Ambient concentrations of species are influenced by its emissions, atmospheric dilution/compaction, chemical loss/production, and wet/dry deposition. As the target sFAs and uFAs in urban environments are predominately primary in their source origin, the chemical production rate could be assumed to be negligible. Donahue et al. (2005) formulated the relative rate expression for heterogeneous oxidation reactions of multicomponent OA. The specific expression applied to the ambient measurements of uFAs is derived, as given in Equation (Eq 1) and Equation (Eq 2) (Wang and Yu, 2021).

$$\frac{c_i}{c_s} = A \times e^{-kt} \qquad (1)$$

$$k \approx k_{r_i} \times C_{OX} \qquad (2)$$

$C_i$ and $C_s$ are the particle-phase concentration of species $i$ and sFAs, respectively. Among the quantified sFA and uFA cooking markers, palmitic acid was selected as the reference molecule for normalization. Using the concentration ratio eliminates the interference from atmospheric dilution and deposition. Fitting the ambient $C_i/C_s$ data versus $t$ with an exponential function provides an estimate for $k$, the effective pseudo-first order decay rate (h$^{-1}$). $k_{ri}$ is the second-order reaction rate constant of species $i$ against an oxidant. $C_{OX}$ is the average oxidant concentration in the aerosol.

**2.4 Source apportionment based on PMF**

Positive Matrix Factorization (PMF) is a bilinear factor analysis method, which is widely used to identify pollution sources and quantify their contributions to the ambient air pollutants at receptor sites, with an assumption of mass conservation between emission sources and receptors (Amato et al., 2009; Lee et al., 2008). In this study, the United States Environmental Protection Agency (USEPA) PMF version 5.0 (Norris et al., 2014) was applied to perform the analysis. PMF decomposes the measured data matrix, $X_{ij}$, into a factor profile matrix, $f_{kj}$, and a factor contribution matrix, $g_{ik}$, (Eq 3):

$$x_{ij} = \sum_{k=1}^{p} g_{ik} f_{kj} + e_{ij} \qquad (3)$$

$$Q = \sum_{i=1}^{n} \sum_{j=1}^{m} (e_{ij}/u_{ij})^2 \qquad (4)$$

where $X_{ij}$ is the measured ambient concentration of target pollutants; $g_{ik}$ is the source contribution of the $k_{th}$ factor to the $i_{th}$ sample, and $f_{kj}$ is the factor profile of the $j_{th}$ specie in the $k_{th}$ factor; $e_{ij}$ is the residual concentration for each data point. PMF seeks a solution that minimizes an object function $Q$ (Eq 4), with the uncertainties of each observation ($u_{ij}$) provided by the user.

The uncertainty of each data point was calculated according to Eq 5:

$$u_{ij} = \sqrt{(x_{ij} \times EF)^2 + (\frac{1}{2} \times MDL)^2} \qquad (5)$$

where MDL is the method detection limit and $EF$ is the error fraction determined by the user and associated with the measurement uncertainties. The concentration data below MDL was replaced by 0.5 of the MDL, and the corresponding uncertainty $u_{ij}$ was calculated by five-sixths of the MDL. Missing values were replaced by the median value of the species, and its $u_{ij}$ was assigned as four times of the median value (Norris et al., 2014).

**3. Results and discussion**

The time series of hourly data of meteorological parameters, gaseous pollutants (including $O_3$ and $NO_2$), $PM_{2.5}$, water soluble ions, carbon components during the monitoring period (January 10-14, February 9-15 and March 11-16, 2021) are shown in Fig.2. During the campaign, the average temperature (T), relative humidity (RH) and wind speed (WS) was 10.9 ±4.5 ℃, 55.3±18.2% and 1.2±0.5 m/s, respectively. The average concentrations of gas pollutants, $PM_{2.5}$, water soluble ions and OC/EC are listed in Table S2. The average concentrations of $NO_2$, $O_3$ and $PM_{2.5}$ were 42.85±25.89, 51.53±29.62 and 50.07±26.54 μg/m$^3$, respectively. Additionally, the average OC and EC concentrations were 6.57±4.63 and 2.12±2.04 μg/m$^3$ respectively, with the contribution of OC to $PM_{2.5}$ ranging from 4.7% to 26.8% (13.2% as average).

179
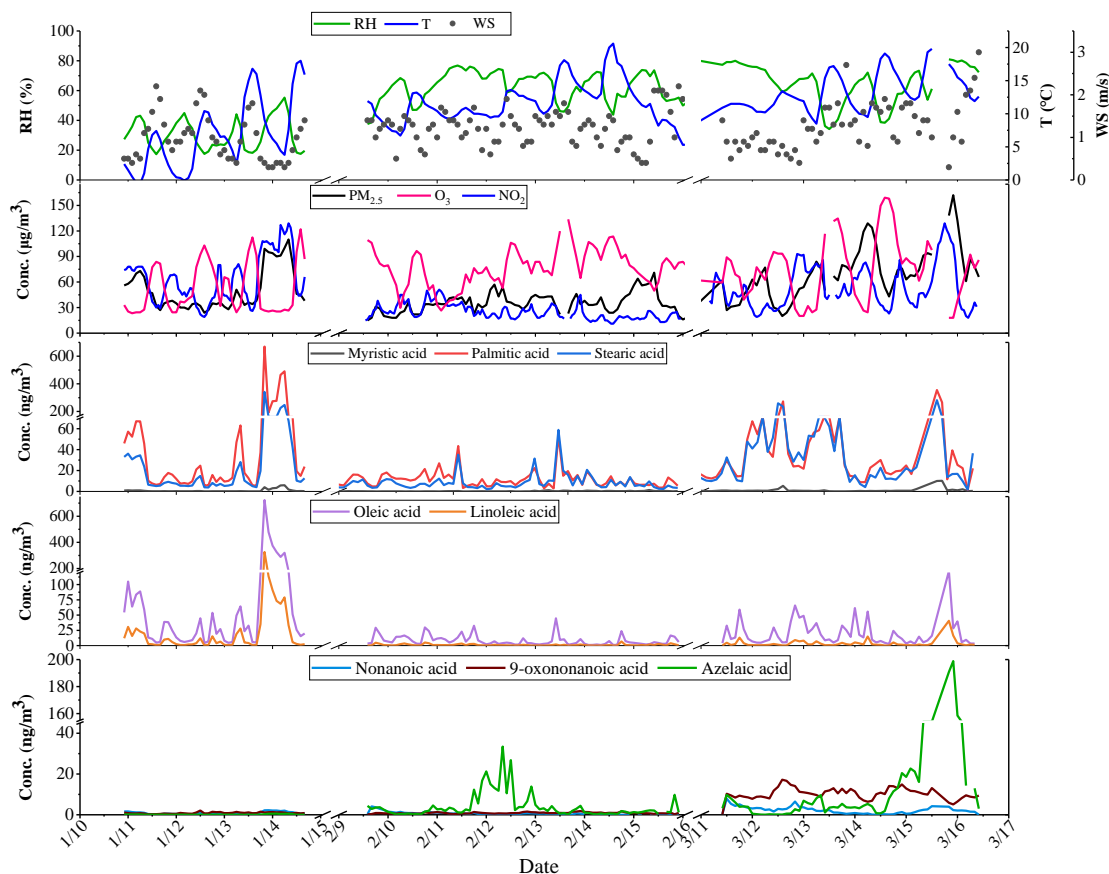
**Figure 2. Time series of pollutants concentration and meteorological parameters**

### 3.1 Characteristics of cooking-derived organic molecular markers

The fatty acids studied include three most abundant sFAs (myristic, palmitic and stearic acids) and two abundant uFAs (oleic and linoleic acids). The concentration of total fatty acids (TFAs, sum of the concentrations of the five fatty acids) was (105.70±230.28) ng/m$^3$, ranging from 8.30 to 2066.30 ng/m$^3$, which is close to the concentrations at the urban site in Shanghai (105 ng/m$^3$) (Li et al., 2020; Wang et al., 2020). The average percentage of TFAs in OC was 1.3% with the maximum value of 8.7% (The concentration of PM$_{2.5}$ at the corresponding time was 99 μg/m$^3$), which was 6.6 times higher than the average. It revealed that the composition of PM$_{2.5}$ could dramatically change, especially during the dinner time (18:00-20:00). The mean concentration of TFAs at dinner time was 172.89 ng/m$^3$, and the contribution of TFAs to PM$_{2.5}$ and OC mass concentration was 2.7‰ and 1.8%, respectively, which were 1.6 and 1.4 times of the mean during the observation period.

We define the "polluted period" as the periods with hourly PM$_{2.5}$ concentrations exceeding 35 μg/m$^3$, and the remaining periods are defined as "clean period". Table 2 shows the mean values of PM$_{2.5}$, OC, TFAs concentrations and meteorological conditions during the clean (PM$_{2.5}$ <35μg/m$^3$) and polluted periods (PM$_{2.5}$ ≥35μg/m$^3$). Generally, the

194  meteorological conditions during the polluted period are unfavourable compared to the clean period, showing lower wind

195  speed and higher humidity. The ratios of WS, T and RH during the polluted period to the clean period are 0.9, 1.0 and 1.1

196  respectively. The mean concentration of $PM_{2.5}$ during the polluted period was 62.86 μg/m$^3$, which was 2.2 times higher

197  than that during the clean period (28.29 μg/m$^3$). OC and $PM_{2.5}$ were similar, with concentrations during the pollution period

198  being 2.0 times higher than during the clean period. The mean concentration of TFAs in the polluted period was 147.06

199  ng/m$^3$, 4.2 times higher than that in the clean hours (35.28 ng/m$^3$). Additionally, the concentrations of sFAs and uFAs in

200  the polluted hours were 4.3 and 4.1 times higher than those during the clean period, respectively.

201  The concentration of TFAs were influenced by emissions, accumulation, transport and dispersion of pollutants during

202  the polluted periods (Hou et al., 2006; Schauer et al., 2003). The fatty acid content of 1.95 ng/μg in $PM_{2.5}$ during the

203  polluted period was 1.6 times greater than that of 1.24 ng/μg during the clean period, which was smaller than the variation

204  range of $PM_{2.5}$ and OC concentrations before and after the polluted period. The variation of TFAs in OC was similar to that

205  in $PM_{2.5}$. Table S1 shows the contribution of total fatty acids directly emitted from various sources to OC, in which the

206  contribution of TFAs from vehicle exhaust is the least, and the proportion of TFAs emitted from cooking in OC is higher

207  than that from other sources. The change in TFAs/OC was weaker than the change in OC, mainly because cooking has

208  relatively small fluctuations in emissions, while the increase in OC concentration was more significant with simultaneous

209  contributions from other sources (e.g., biomass burning, coal combustion, and vehicle exhaust). Similarly, the mass

210  concentration of $PM_{2.5}$ was driven by emission source significantly. The observed contribution of TFAs to OC in $PM_{2.5}$ was

211  smaller than TFAs/OC ratio in cooking, but larger than that in other sources.

212  **Table 2. $PM_{2.5}$ concentration, organic carbon fraction, fatty acids concentration and meteorological conditions during clean**

213  **and polluted periods.**

| Species | Clean period | Polluted period | Polluted/clean |
|---|---|---|---|
| $PM_{2.5}$ (μg/m$^3$) | 28.29 ± 5.27 | 62.86 ± 25.67 | 2.2 |
| OC (μg/m$^3$) | 4.05 ± 1.09 | 8.00 ± 5.23 | 2.0 |
| TFAs (ng/m$^3$) | 35.28 ± 28.17 | 147.06 ± 281.66 | 4.2 |
| sFAs (ng/m$^3$) | 21.60 ± 14.91 | 92.05 ± 162.75 | 4.3 |
| uFAs (ng/m$^3$) | 13.68 ± 14.22 | 55.53 ± 133.82 | 4.1 |
| TFAs/$PM_{2.5}$ (ng/μg) | 1.24 ± 0.91 | 1.95 ± 2.85 | 1.6 |
| TFAs/OC (ng/μg) | 9.52 ± 7.79 | 15.33 ± 14.59 | 1.6 |
| WS (m/s) | 1.23 ± 0.45 | 1.14 ± 0.54 | 0.9 |
| T (℃) | 10.77 ± 4.22 | 10.99 ± 4.68 | 1.0 |
| RH (%) | 53.41 ± 17.49 | 56.33 ± 18.55 | 1.1 |

214  Similar variation and diurnal patterns were found for these five fatty acids (Fig.3), confirming their common origin.

215  In addition, compared to fatty acids, the time series of $C_9$ acids showed a different diurnal variation, suggesting different

production and reaction processes. Fatty acids showed a clear diurnal variation, with two peaks observed at around 6:00

and 20:00 local time, respectively, and the dinner time peak was especially prominent. In contrast to the previous

observations in Shanghai, no peak was observed at lunchtime. The relatively higher boundary layer during the daytime,

facilitated the diffusion of pollutants. The weaker oxidation of uFAs emitted at night made the fatty acid concentration

peaks more pronounced at dinner time (Wang et al., 2020). Figure 3(b) shows the contribution of various fatty acids to OC.

From the diurnal patterns, it is shown that the proportion of the five fatty acids and TFAs in OC at noon had a weaker peak,

which was still smaller than that during the morning and evening mealtimes. In conclusion, the apparent peaks of TFAs at

the dinner time provide evidence for major source contribution to air pollution from local cooking emissions, although

there are mix sources including vehicle exhaust, coal combustion, etc.
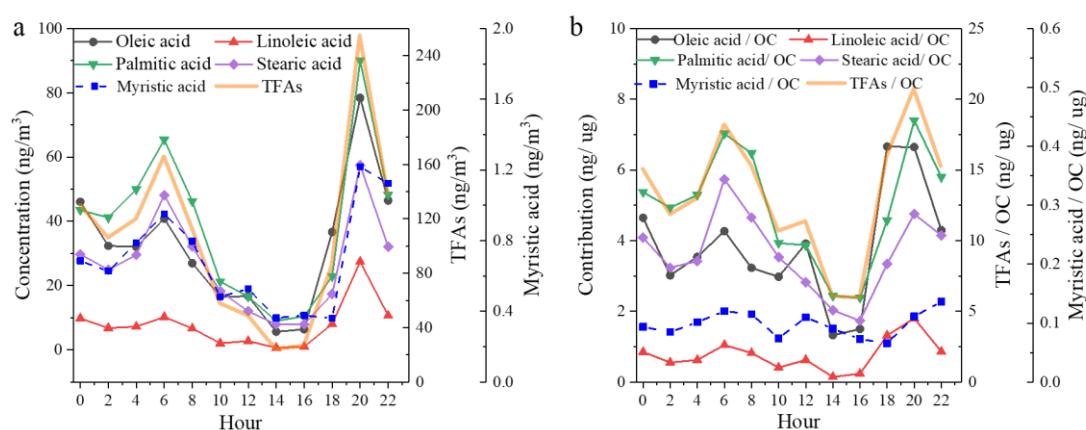
**Figure 3. Diurnal variation of five fatty acids and TFAs during the observation period.**

Fatty acids in urban atmospheres are influenced by various anthropogenic (e.g., biomass burning, vehicle exhaust)

(Hays et al., 2002; Schauer et al., 2001; Simoneit, 2002; Wang et al., 2009) and biogenic sources (Oliveira et al., 2007;

Rogge et al., 2006). The main sources of fatty acid-like substances in the ambient air of the study area can be discerned on

the basis of characteristic ratios between fatty acids emitted from different sources (Fig.4) (He et al., 2004; Pei et al., 2016;

Rogge et al., 1993; Zhao et al., 2015; Zhao et al., 2007). The palmitic acid to stearic acid (P/S) ratios observed in this study

ranges between 0.49 and 3.08 (average value: 1.49), significantly lower than those associated with residential coal

combustion and industrial coal combustion, while partially overlapping those from biomass burning, vehicle exhaust and

sea spray aerosol (Bikkin et al., 2019; Cai et al., 2017; Ho et al., 2015; Zhang et al., 2008; Zhang et al., 2007). Ho et al.

(2015) investigated urban areas in Beijing where fatty acid concentrations were elevated during traffic restrictions

compared to non-restricted periods, suggesting that motor vehicle exhaust is not the largest source of fatty acids in urban

areas. The information on fatty acid emissions from biomass burning source is closer to that of cooking sources (Hays et

al., 2002; Schauer et al., 2001; Zhang et al., 2008), however, in the study of Simoneit (2002), no oleic acid was detected in organic molecular substances from biomass burning. The oleic acid/stearic acid (O/S) ratio from sea spray aerosol samples is 0.16 (Bikkin et al., 2019), which is obviously lower than the ambient data in this study (1.4). Hence, during the observation in this study, vehicle exhaust and sea spray were not the most important sources of fatty acids emissions in urban Changzhou. Especially during the dinner period, when the O/S ratio was significantly higher and close to the ratio in the organics emitted from traditional culinary types in the Yangtze River Delta region.
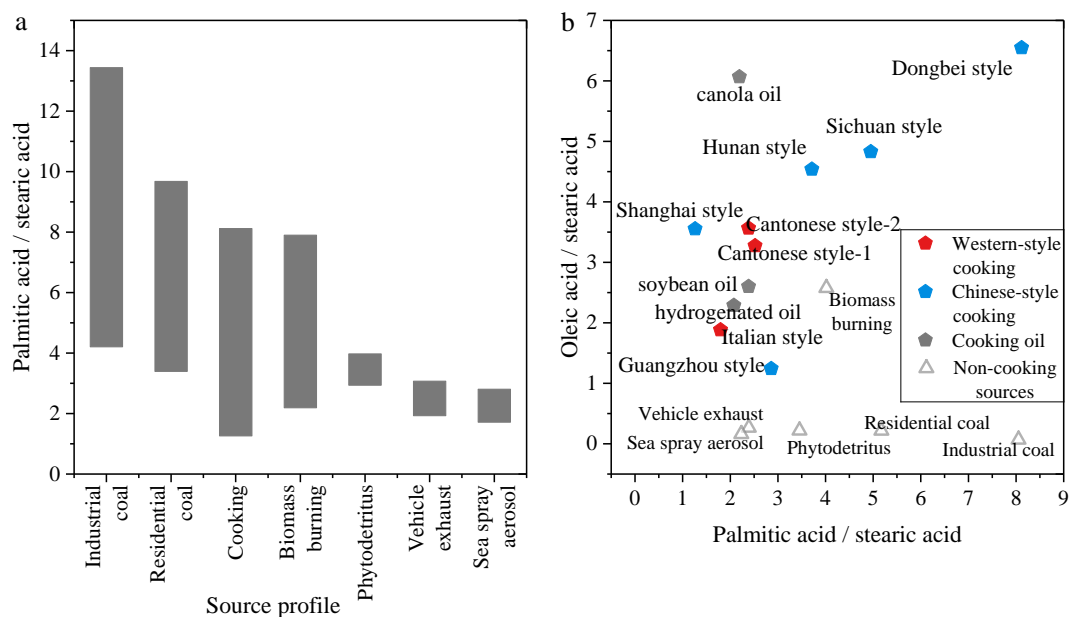
**Figure 4. Ratio of fatty acids (P/S) in organic molecular substances emitted directly from different sources (a); Ratio of fatty acids (P/S vs O/S) emitted by different types of cooking sources and non-cooking sources (b). (Bikkin et al., 2019; Cai et al., 2017; Hays et al., 2002; He et al., 2004; Oliveira et al., 2007; Pei et al., 2016; Rogge et al., 1993; Schauer et al., 2001; 2002; Simoneit, 2002; Zhang et al., 2008; Zhao et al., 2007).**

Information on the changes of specific molecular markers is useful in investigating the aging process of aerosol. The two uFAs (oleic acid and linoleic acid) are more reactive with atmospheric oxidants (OH and $O_3$, etc.) in the atmosphere due to the presence of C=C bonds, compared to sFAs. Furthermore, the two homologous sFAs (palmitic and stearic acid) have similar chemical structures, reactivity and volatility, thus their concentration ratios can be assumed to remain constant during post-emission periods. Therefore, the ratio of P/S mainly depends on the sources. Fig.5 shows the O/S ratios and linoleic acid/ stearic acid (L/S) versus P/S, respectively. The average value of P/S was 1.49±0.49, which was within the range of cooking source profile values measured from direct emissions from different restaurants and cooking types (1.3-8.1) (He et al., 2004; Pei et al., 2016; Schauer et al., 2002; Zhao et al., 2007), and similar to the ratio of P/S in atmospheric PM2.5 in Shanghai (1.9) (Li et al., 2020; Wang et al., 2020). In this study, the O/S ratio (1.4 ± 1.1) of the ambient samples was overall in the range of the cooking source profile (3.6 ± 1.6), while the L/S ratio of 0.25 ± 0.31 was slightly lower than

259  the cooking source profile values (2.9 ± 1.8) (He et al., 2004; Pei et al., 2016; Schauer et al., 2002; Zhao et al., 2007). The

260  results of Moise and Rudich (2002) showed that the reactant activity is directly related to the concentration of unsaturated

261  bonds, with linoleic acid having an extra double bond than oleic acid, indicating that linoleic acid is more easily degraded

262  than oleic acid (Moise and Rudich, 2002; Thornberry and Abbatt, 2004). The O/S ratio of the ambient samples in this study

263  was higher than those measured in Beijing (0.65) (He et al., 2004) from January to October and in Shanghai (0.83) (Li et

264  al., 2020; Wang et al., 2020) during winter.

265      The diurnal variations of O/S and L/S are also shown in Fig.5. The ratios were significantly higher during dinner time,

266  and were closer to the cooking source profile. Demonstrating that changes in fatty acid concentrations may be influenced

267  primarily by cooking source emissions, especially during dinner time when fresh cooking source emissions entered into

268  the atmosphere and uFAs were quickly consumed due to aging. The ratio of linoleic acid to stearic acid is consistently

269  lower than what is involved in the source spectrum, which may be influenced by different regions and source characteristics

270  from different types of restaurants, as well as small emissions from other minor sources.
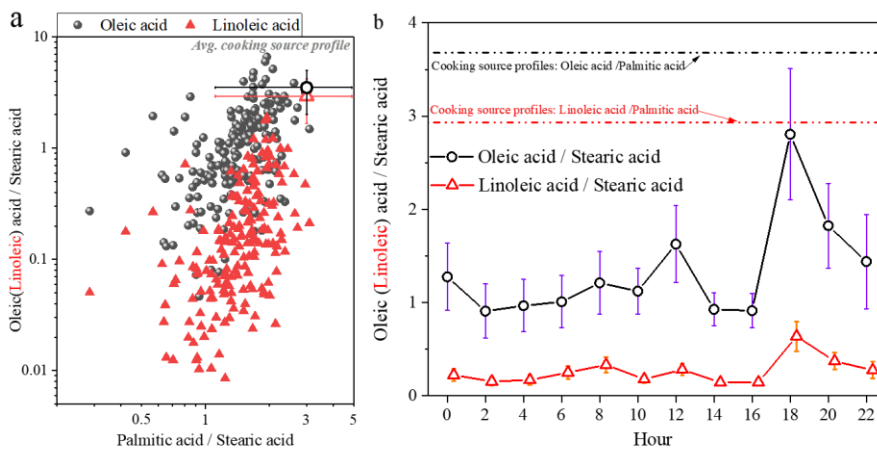
271

272  **Figure 5. The oleic/ stearic acid and linoleic/ stearic acid ratios compared to the palmitic/stearic acid ratio (a); diurnal variation**

273  **in the ratio of oleic (linoleic) acid to stearic acid concentration (b). (The cooking source profile values were measured from direct**

274  **emissions from different restaurants and cooking types.) (He et al., 2004; Pei et al., 2016; Schauer et al., 2002; Zhao et al., 2007).**

275  **3.2 Backward trajectory clustering analysis**

276      The best solution of four clusters was determined based on the variation of the total spatial variance (Fig.6 and Fig.

277  S2). Fig.7 shows the four cluster solutions and the mean distribution of meteorological conditions and pollutants in each

278  cluster. Briefly, cluster #1 (CL#1), which represents 15.4% of the sample, comes from the northwest continental region of

279  China and reaches Changzhou before passing Gansu, Shan'xi and Henan provinces, and the lower temperature and

280  humidity associated with this cluster are consistent with its geographic origin. Cluster #2 (CL#2), which accounts for 35.6%

281  of the total number of trajectories, represents air masses from the northeastern part of the ocean, and the temperature and

282 humidity associated with this cluster are higher than those of CL#1. Cluster 3 (CL#3), contributing 18.6%, traveling slowly

283 from inland area, is associated with the lowest wind speed, with higher temperature and humidity than CL#1 but lower

284 than CL#2. Cluster 4 (CL#4), representing 30.3% of the trajectories, represents the eastern/southeastern oceanic air masses,

285 with the highest observed temperature, humidity and wind speed among all of the air masses. CL#2 and CL#4 have

286 relatively high temperature, humidity and wind speed. CL#3 is associated with the highest $NO_2$ concentrations, confirming

287 its local air mass origin, and the $PM_{2.5}$ and OC concentrations in this air mass are also the highest compared to all the other

288 air masses.

289       The concentrations of sFAs, uFAs and their oxidation products under each cluster are shown in Fig.6. The total

290 concentrations of sFAs, uFAs and uFAs' oxidative decomposition products (ODPs, in this study, ODPs includes azelaic

291 acid, nonanoic acid and 9-oxononanoic acid) within the four types of air mass clusters were in the order of

292 CL#3>CL#2>CL#4>CL#1, where the TFAs in CL#1 and CL#3 were larger than the percentages in CL#2 and CL#4. The

293 relative contents of sFAs and uFAs in CL#1 and CL#3 are closer than those in the other two types of air masses, and are

294 closer to the concentration ratio of the species directly emitted from the cooking source (the value of uFAs /sFAs range

295 from 0.8 to 3.2) (He et al., 2004; Pei et al., 2016; Schauer et al., 2002; Zhao et al., 2007), which indicated that the oxidative

296 decomposition of uFAs is less in CL#1 and CL#3. CL#3 was a slowly moving, local cluster. Under this air mass clustering,

297 local emissions contribute significantly to fatty acids as well as $PM_{2.5}$ concentration. The air mass of CL#1 exhibits the

298 longest range, the concentrations of ODPs were relatively small among all air masses, and the low ODPs concentration

299 was inconsistent with other literature findings of more aging aerosol production from long-range transport (Wang et al.,

300 2020). The lowest $PM_{2.5}$ concentrations and cleaner air masses during air mass CL#1 suggested that long-range air mass

301 transport from the northwest was not the main source of fatty acids and ODPs in Changzhou during the observation. The

302 value of uFAs /sFAs in CL#2 and CL#4 was less than that in CL#1 and CL#3 and less than the ratio in sources. In addition,

303 the proportion of ODPs in CL#2 and CL#4 is greater than that in CL#1 and CL#3. This result may be explained by the

304 following two reasons: first, under the influence of transport, the air masses brought more sFAs, ODPs, and the air masses

305 were more aged, for example, marine heterotrophic bacteria releases sFAs and uFAs into the water column, however the

306 mono/polyunsaturated fatty acids (e.g., oleic acid, linoleic acid) in seawater rapidly oxidizes to form initially oxocarboxylic

307 acids, azelaic acid etc. (Bikkin et al., 2019); second, under the influence of CL#2 and CL#4 air masses, in which the ozone

308 concentration was higher than other air masses, the decomposition reaction of uFAs was more active and could produce

309 more ODPs. In addition, the oxidative reaction of uFAs could be influenced by meteorological conditions as well.
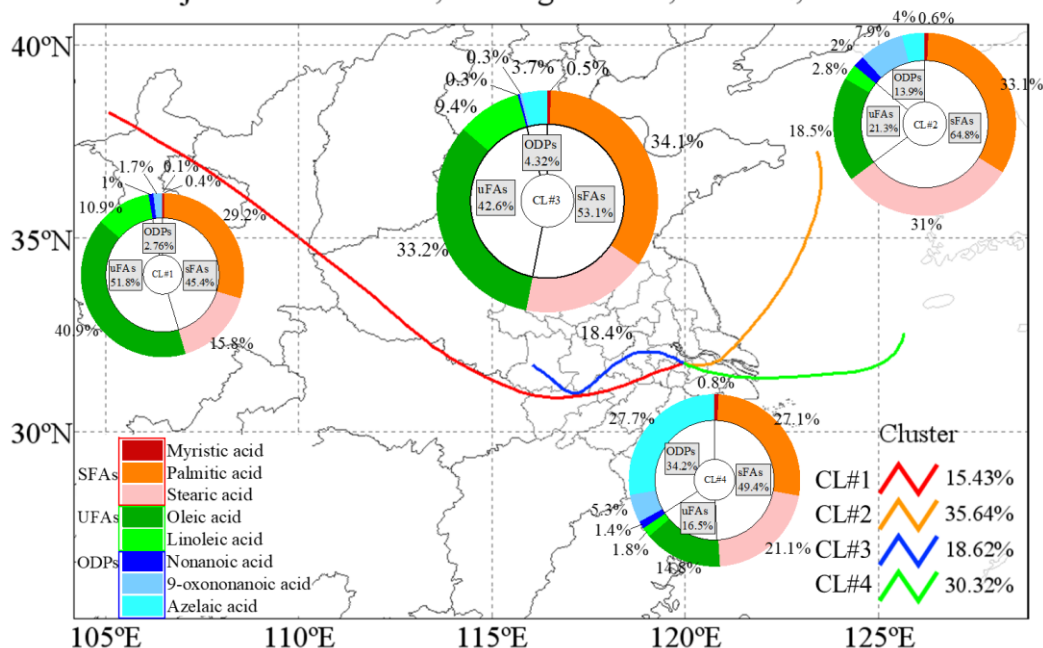
**Figure 6. Sources for each air mass during the sampling period. The colord lines in the map show the contribution of each directional air mass source to the total trajectory as resolved by the TrajStat model.**
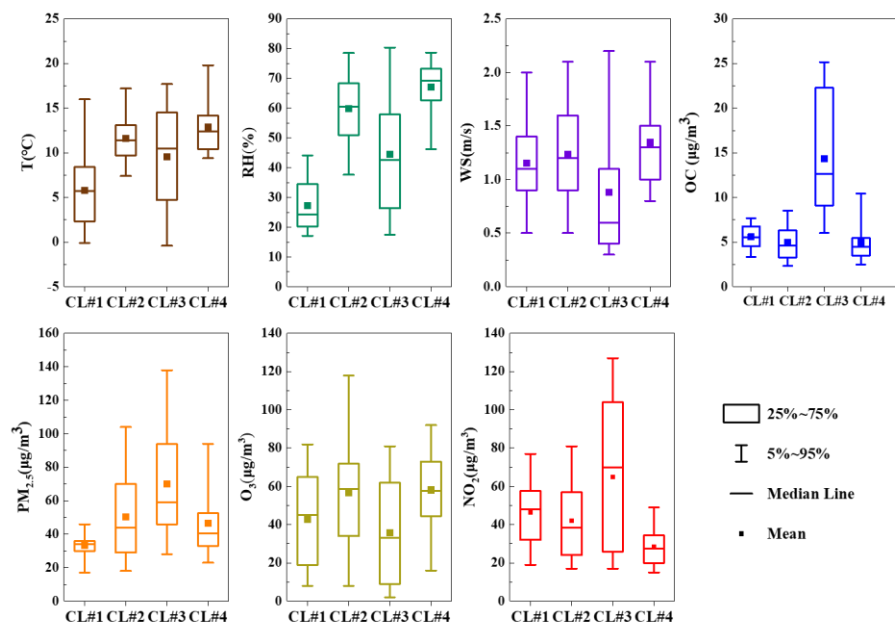
**Figure 7. Box plots of meteorological parameters and pollutant concentrations in each cluster (squares and solid lines correspond to the mean and median, respectively; boxes indicate the 25th and 75th percentiles, whiskers are the 5th and 95th percentiles).**

**3.3 Atmospheric aging of unsaturated fatty acids**

Fig.8(a) shows the diurnal variation of ozone, oleic acid, and ODPs. The ozone concentration started to rise in the morning (06:00) and peaked in the late afternoon (14:00). The diurnal trend of oleic acid was opposite to that of ozone. The diurnal trend of ODPs was also different from oleic acid, the small peak of ODPs was found at around 12:00 in the

daytime, which was earlier than that of ozone. At the same time, oxidative decomposition, atmospheric dilution and lower

emissions caused significant decrease in the concentration of oleic acid until night when large amounts of fresh emissions

enter the atmosphere again. The decreasing rate of oleic acid concentration slowed down around noon, probably because

of fresh emission (e.g., cooking source) at lunch time. C9 ω-oxo acid and diacids (e.g., nonanoic acid, 9-oxononanoic acid

and azelaic acid) in the atmospheric environment originate from plant volatilization, combustion emissions, and cooking

processes (Kawamura et al., 2013; Tian et al., 2020), and they were established in chamber studies as major atmospheric

oxidation products from uFAs ozonolysis (Kawamura et al., 2013; Moise and Rudich, 2002; Thornberry and Abbatt, 2004).

The diurnal variations of Nonanoic acid and 9-oxononanoic acid were similar and both peaked around noon, while the

production of 9-oxononanoic acid and azelaic acid are in competition (Thornberry and Abbatt, 2004). However, the

concentration of 9-oxononanoic acid was significantly higher than that of nonanoic acid (Fig.8, c and d), which may be

due to the following reasons: (1) 9-oxononanoic acid can be produced by two pathways, while nonanoic acid generation

can only be produced through one of the pathways competing with nonanal, and the molarity generated from the ozonolysis

of oleic acid is smaller than that of 9-oxononanoic acid (Gross et al., 2009); (2) due to the high volatility of nonanoic acid,

its concentration in the particle phase is much lower, and only a small portion of nonanoic acid in PM is detected by TAG

(Wang and Yu, 2021).
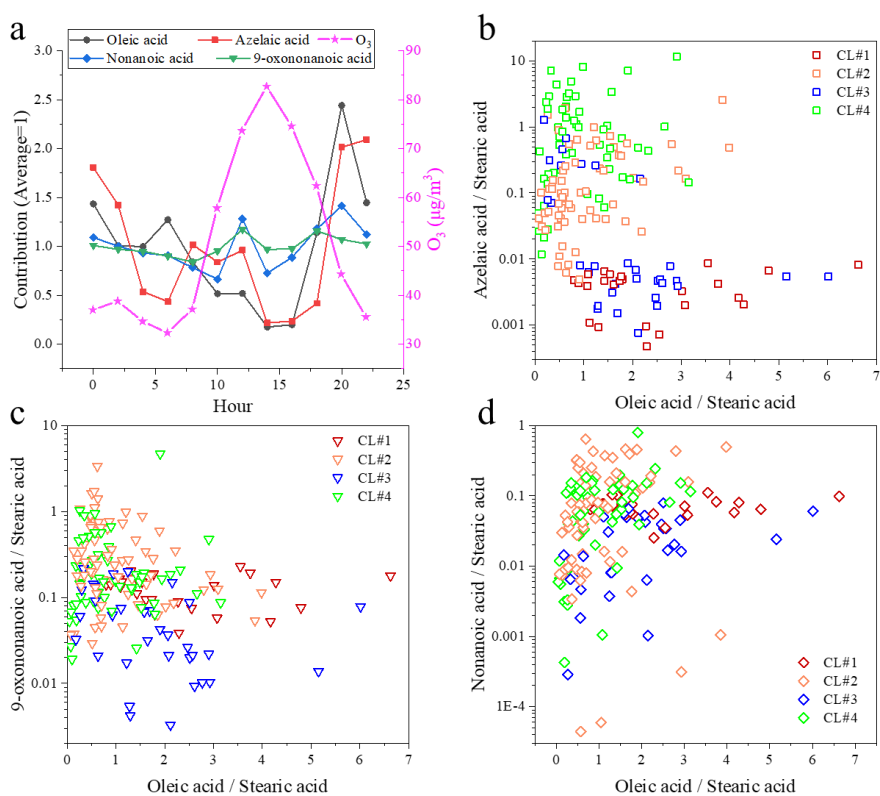
**Figure 8. Diurnal variation of C9 products and oleic acid in environmental samples compared to O₃ (a); Correlation of C9**

**products azelaic acid (b), 9-oxononanoic acid (c), and nonanoic acid (d) with oleic acid.**

Fig.8(b) to (d) show the relationship between ODPs / stearic acid ratio and oleic acid/stearic acid. In CL#2 and CL#4, 9-oxononanoic acid / stearic acid ratio is larger than that in CL#1 and CL#3, and azelaic acid /stearic acid ratio have the same characteristic. The nonanoic acid / stearic acid ratio is not well characterized, probably because most of the nonanoic acid is present in the gas phase. Bikkina et al. (2019) found that the O/S ratio exhibited a nonlinear (power) inverse relationship with azelaic acid in remote marine aerosols. This feature was not found in this study, which is possibly due to the single source class of fatty acids and ODPs in remote marine areas, the diversity of emission sources in urban areas, and their vulnerability to transport.

## 3.4 Oxidative decomposition of uFAs

From the above analysis, cooking emission was the most important source of fatty acids in atmospheric $PM_{2.5}$ in urban areas of Changzhou, especially during the dinner period. Both sFAs and uFAs peaked between 18:00 and 22:00 pm, and then declined until breakfast time in the next day. Fatty acid-like substances in fresh cooking emissions react with various oxidants while being continuously replenished by the fresh cooking emission during the day so that the degradation of uFAs in the particulate phase can be complicated. With no obvious fresh cooking emissions after dinner, and the low volatility of the target pollutants studied (oleic and linoleic acids), the effect of gas-particle partitioning on them can be disregarded, and the evening provides a good opportunity to investigate the chemical degradation of uFAs from cooking emissions. Therefore, we selected the period from 18:00 in the evening to 6:00 in the morning, focusing on the impact of oxidants in the atmospheric environment on uFAs. The definition of the effective rate constant $k$ has been described in previous studies (Donahue et al., 2005; Wang and Yu, 2021). To calculate the rate constant of uFAs with oxidants (especially $O_3$ and $NO_3^*$, etc), a one-step model was utilized, and an average decay rate constant at each night could be derived. The same method has been used in the study of Wang and Yu (2021), which shows that more than 77% of the observed data fits better with a one-step model. Figures S5 and S6 show the night-time oxidative degradation of oleic acid and linoleic acid, respectively. It should be noted that not all of the reactants (uFAs) will be fully consumed from the start of the fit until fresh emissions enter the atmosphere, and the amount of consumed and remaining uFAs could be affected by a combination of oxidant level, source activity, and meteorological conditions.

Fig.9 shows the effective rate constants of the oxidative decomposition of oleic ($k_O$) and linoleic ($k_L$) acids in relation to air oxidants ($O_3$, $NO_2$, $O_x$ and $NO_3^*$, etc. $O_x$ is the total oxidant, calculated from $O_x = NO_2 + O_3$.). It should be noted that the $NO_3^*$, calculated by multiplying $O_3$ by $NO_2$, is a substitution for $NO_3^*$ radical, which is not available in this campaign.

366    Both $k_O$ and $k_L$ had a significant positive correlation (The P values of significance tests were all less than 0.05) with $O_3$,

367    and no correlation was observed with other air oxidants ($O_x$, $NO_3^*$ and $NO_2$). Ozone acted as the predominant oxidant for

368    the oxidative decomposition of uFAs, which was consistent with the conclusion in Shanghai. In addition to the oxidants

369    mentioned above, laboratory studies has also reported $N_2O_5$ reacts with olefinic acids containing C=C bonds such as oleic

370    acid and linoleic acid, which has a much slower reaction kinetics than that of $NO_3^*$ (Gross et al., 2009). Therefore, the

371    effect of $N_2O_5$ was ignored in this study.

372    Fig.10 shows the scatter plot of the effective rate constants of oleic and linoleic acid. The significant correlation

373    between the effective rate constants of oleic acid and linoleic acid was not equal to 1 due to the differences in aerosol

374    composition and environmental conditions. The effective rate constant of oleic acid ranged from 0.08-0.57 h$^{-1}$, which was

375    overall smaller than $k_L$ (0.16-0.80 h$^{-1}$), indicating that their reactivity is closely related to their chemical structure, and the

376    two -C=C- bonds in the linoleic make a higher probability in reacting with atmospheric oxidants. However, besides the

377    chemical structure, other factors (e.g., diffusion, and temperature) also affect the calculation of oxidation reaction rate of

378    uFAs. The fitted ratio of $k_L/k_O$ is 1.29 (red dashed line in Fig.11), with most scatters fall in the area with $k_L$ to $k_O$ values

379    above the 1:1. $k_L/k_O$ has a mean value of 1.6 ± 0.3 and the relative reactivity of linoleic acid to oleic acid is below 2 in the

380    measured environmental data, but close to the results of laboratory studies with $O_3$ as oxidant. We also reviewed the $k_L/k_O$

381    ratios of $O_3$, $NO_3^*$ and $N_2O_5$ as oxidants in other laboratory studies, and the $k_L/k_O$ ratios of the three oxidants were 1.7, 1.8

382    and 2.9 (Gross et al., 2009; Thornberry and Abbatt, 2004), respectively. The relative reaction coefficients $k_L/k_O$ measured

383    for $O_3$ in laboratory studies are close to our results. The comparison indicates that $O_3$ was the most likely oxidants for the

384    nighttime uFAs oxidation in the urban area of Changzhou.
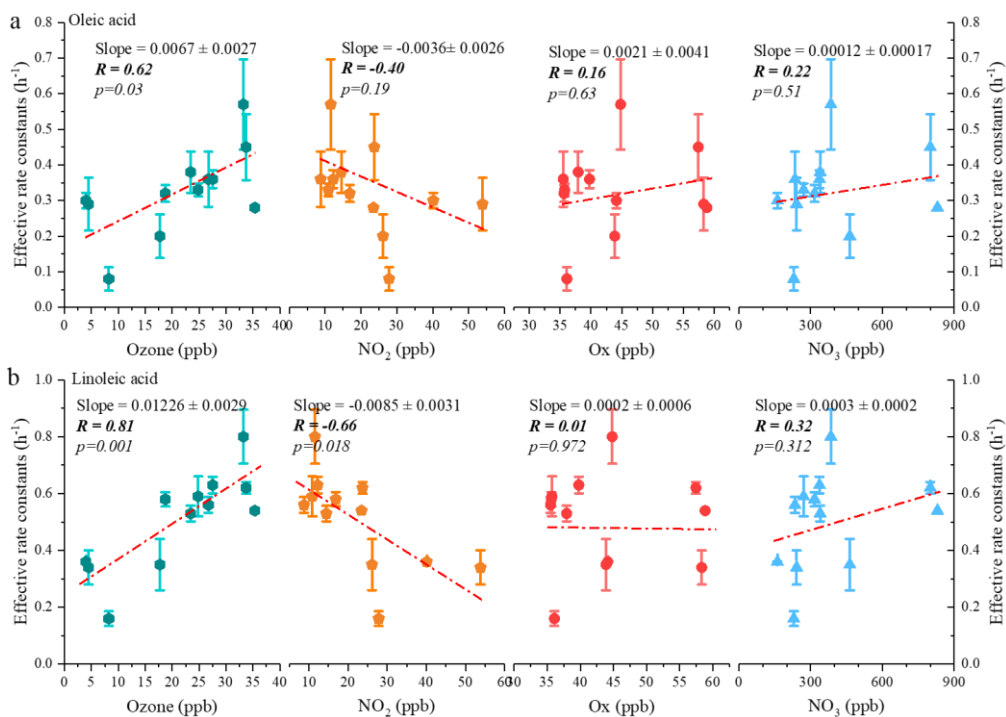
385

386 **Figure 9. Correlations of the estimated effective decay rate constant with average night-time atmospheric oxidants**

387 **concentration for oleic acid (a) and linoleic acid (b). (The p-value indicates the parameter of the F-test of the regression**

388 **equation in the regression model.)**
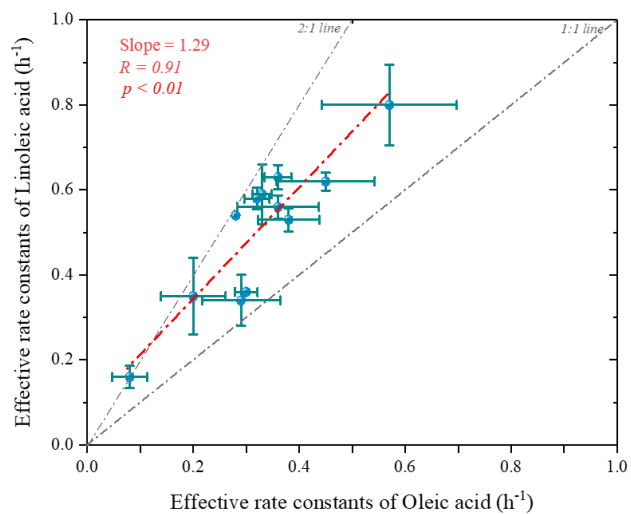
389

390 **Figure 10. Scatter plot of the estimated effective rate constant for linoleic acid versus oleic acid (The p-value indicates the**

391 **parameter of the F-test of the regression equation in the regression model).**

392 **3.5 Source contributions of cooking aerosol to PM$_{2.5}$ and OC**

393       To gain a more quantitative assessment of source contribution from cooking to OA, PMF was applied for source

394 apportionment. The target POA markers were incorporated into the input data matrix, along with SOA markers (Table S1)

395 and major aerosol components including major ions, elements, EC, and OC. Source apportionment of PM$_{2.5}$ in this field

396   campaign yielded 10 sources, including three secondary sources (secondary sulfate, secondary nitrate and SOA,

397   respectively) and seven primary emission sources (cooking, biomass burning, coal combustion, vehicle exhaust, industrial

398   emissions, dust and fire working, respectively). A detailed description of the identification of each PMF-resolved source

399   factor is shown in section S1. Briefly, secondary source factors account for the largest share of $PM_{2.5}$ (the total was 56.9%,

400   of which secondary nitrate contributes up to 34.4%), and primary emissions contributed to 43.1% of total $PM_{2.5}$ (Fig.11).

401   Among the primary source factors, industry makes the largest contribution to $PM_{2.5}$ mass concentration (9.9%).

402     In a specific pollution period, different sources have different impacts on $PM_{2.5}$ concentration and chemical

403   compositions in Changzhou. Among the 10 sources, the cooking factor was dominated by sFAs and uFAs during the

404   monitoring period, accounting for 4.6% of the total $PM_{2.5}$. The concentration of cooking source and its contribution to total

405   $PM_{2.5}$ also showed a clear diurnal variation, with two peaks at around 6:00 and 20:00, respectively, especially at the dinner

406   time. The contribution of cooking to $PM_{2.5}$ concentration during mealtime increased significantly compared with other

407   periods, reaching 7.8% at 20:00. The mean concentration of cooking aerosol in the polluted period was estimated to be 4.0

408   $\mu g/m^3$, which was 5.3 times higher than that in the clean period (0.75 $\mu g/m^3$). The variation was similar to that of fatty

409   acids. The factor profiles of the 10-factor constrained run of PMF are shown in section S1 and Figure S5, together with the

410   time series of contributions from individual source factors. Overall, we estimated that cooking accounted for 5.8% of the

411   total $PM_{2.5}$ during the pollution period, which was 1.9 times greater than that of 3.0% during the clean period. During the

412   whole observation period, the cooking factor contributes only a small part of $PM_{2.5}$ (4.6%), but it accounts for 8.1% of the

413   total OC, indicating the importance of cooking emissions to organic matter, which is a significant source of organic

414   pollution in urban areas.
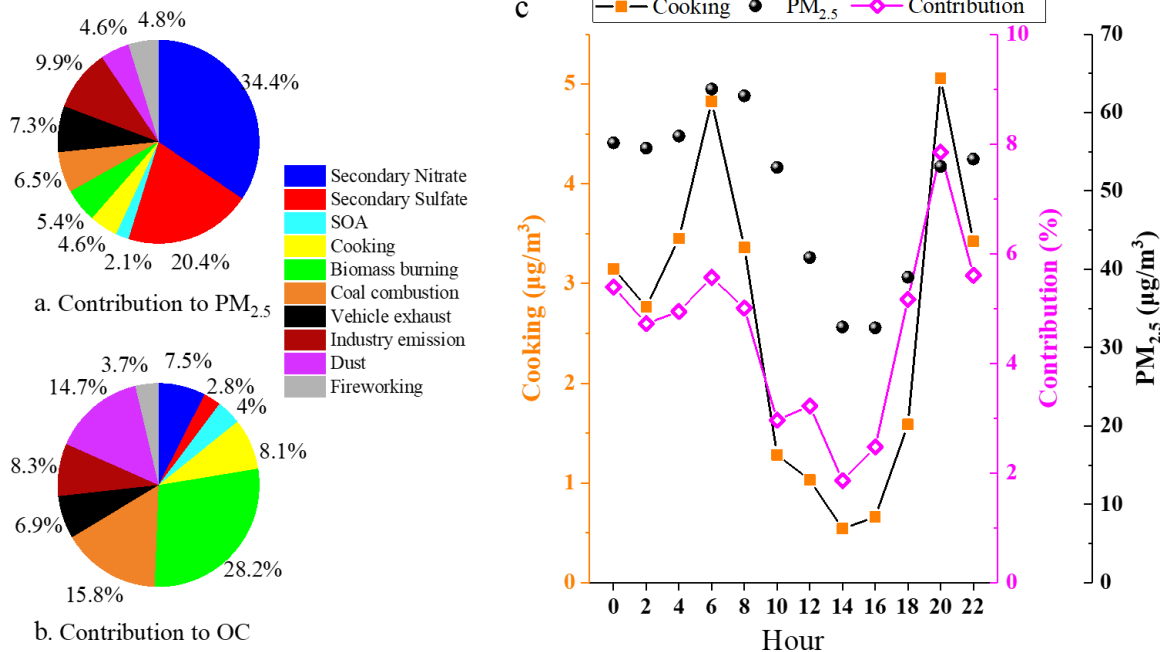
**Figure 11. Comparison of individual factor contributions to PM$_{2.5}$ (a) and OC (b); diurnal variation of cooking source (c).**

## 4. Conclusions

In this study, we measured uFAs, sFAs, and ODPs every two hours using TAG in the urban Changzhou city. The concentration of TFAs averaged at 105.70 ng/m$^3$, close to that in Shanghai. The average concentration of TFAs in polluted period was 147.06 ng/m$^3$, which was 4.2 times higher than that during clean period. During the rising period of PM$_{2.5}$, TFAs concentration tends to reach the peak earlier than PM$_{2.5}$, and the proportion of TFAs in PM$_{2.5}$ as well as OC will increase first and then decrease. However, when affected by adverse diffusion, TFAs concentration will accumulate continuously as PM$_{2.5}$. The linoleic acid /stearic acid and oleic acid /stearic acid ratios exhibited a significant peak during dinner time, which was close to the cooking source profile values, and a relatively smaller peak at lunchtime. Cooking sources during dinner hours are the most important contributors to the concentration of fatty acids in PM$_{2.5}$ during the study period. Diurnal trend of ODPs was different from that of uFAs, and the concentration of ODPs increased significantly at noon. The diurnal variations of nonanoic acid and 9-oxononanoic acid in ODPs are similar, mainly because oleic acid can produce both 9-oxononanoic acid and nonanoic acid in the ozonolysis pathway.

Under the influence of different air masses, there were significant variations in the ratios of various organic acids from cooking. Highest total concentrations of sFAs, uFAs and ODPs were found under the local air mass cluster (CL#3), indicating significant local emissions contributing to fatty acids as well as PM$_{2.5}$. And the percentages of TFAs in CL#1 and CL#3 were larger than that in CL#2 and CL#4. The proportion of ODPs in CL#2 and CL#4 was greater than that in CL#1 and CL#3. This is mainly because under the influence of transportation, the air masses brought more sFAs, ODPs.

434    The air masses were more aged, and the higher ozone concentration and more active uFAs decomposition reaction occurred

435    in these two air mass clusters. The daily oxidative degradation kinetics of oleic and linoleic acids were obtained using data

436    during night time of each observation date. The $k_O$ ranged from 0.08 to 0.57 $h^{-1}$, which was overall smaller than $k_L$ (0.16-

437    0.80 $h^{-1}$). It was observed that both $k_O$ and $k_L$ had a significant positive correlation with $O_3$. The relative reaction coefficients

438    $k_L/k_O$ (1.6 ±0.3) of linoleic and oleic acids in this study are close to $k_L/k_O$ measured for $O_3$ in laboratory studies, indicating

439    that $O_3$ was the main night-time oxidants for uFAs in Changzhou City. Overall, this study describes the concentration

440    variation and oxidative degradation of uFAs and oxidation products in ambient air based on hourly time-resolved

441    observations, guiding future refinement of source apportionment of $PM_{2.5}$ and the development of cooking emission control

442    policies.

443    The average contribution of cooking to $PM_{2.5}$ was estimated to be 4.6%, while the average contribution to total OC

444    was 8.1%. However, the proportion of cooking to total $PM_{2.5}$ among different sources during the meal period increased

445    significantly compared with other periods, especially during the dinner period, peaking at 7.8%. It is estimated that cooking

446    source accounted for 5.8% of the total $PM_{2.5}$ during the pollution period, which was 1.9 times greater than the 3.0% during

447    the clean period, showing that strict control on cooking emissions should be paid more attention during pollution episodes.

448

449    **ACKNOWLEDGEMENTS**

450    This study is financially supported by the National Natural Science Foundation of China (NO. 41875161, 42075144 and

451    42005112). We thank Changzhou Environmental Monitoring Center of Jiangsu Province to help conduct the field

452    campaign.

453    **AUTHOR CONTRIBUTIONS**

454    RL, KZ, QL and LMY conducted the field measurements. RL and KZ performed the data analysis and prepared the

455    manuscript with contributions from all co-authors. LL formulated the research goals and edited and reviewed the

456    manuscript. LL and JZY reviewed and edited the manuscript. All authors contributed to data interpretations and discussions.

457    **COMPETING INTERESTS**

458    The authors declare no conflict of interest.

459    **DATA AND CODE AVAILABILITY**

460    This paper does not report original code. Data is available from the corresponding author (Lily@shu.edu.cn) upon request.

461    **REFERENCES**

462  Amato, F., Pandolfi, M., Escrig, A., Querol, X., Alastuey, A., Pey, J., Perez, N., and Hopke, P. K.: Quantifying road
463  dust resuspension in urban environment by Multilinear Engine: A comparison with PMF2, Atmos. Environ., 43(17), 2770-
464  2780, doi:10.1016/j.atmosenv.2009.02.039, 2009.

465  Bertrand, A., Stefenelli, G., Jen, C. N., Pieber, S. M., Bruns, E. A., Ni, H. Y., Temime-Roussel, B., Slowik, J. G.,
466  Goldstein, A. H., El Haddad, I., Baltensperger, U., Prevot, A. S. H., Wortham, H., and Marchand, N.: Evolution of the
467  chemical fingerprint of biomass burning organic aerosol during aging, Atmos Chem Phys, 18(10), 7607-7624,
468  doi:10.5194/acp-18-7607-2018, 2018a.

469  Bertrand, A., Stefenelli, G., Pieber, S. M., Bruns, E. A., Temime-Roussel, B., Slowik, J. G., Wortham, H., Prevot, A.
470  S. H., El Haddad, I., and Marchand, N.: Influence of the vapor wall loss on the degradation rate constants in chamber
471  experiments of levoglucosan and other biomass burning markers, Atmos Chem Phys, 18(15), 10915-10930,
472  doi:10.5194/acp-18-10915-2018, 2018b.

473  Bikkin, P., Kawamura, K., Bikkina, S., Kunwar, B., Tanaka, K., and Suzuki, K.: Hydroxy Fatty Acids in Remote
474  Marine Aerosols over the Pacific Ocean: Impact of Biological Activity and Wind Speed, Acs Earth Space Chem, 3(3), 366-
475  379, doi:10.1021/acsearthspacechem.8b00161, 2019.

476  Cai, T. Q., Zhang, Y., Fang, D. Q., Shang, J., Zhang, Y. X., and Zhang, Y. H.: Chinese vehicle emissions characteristic
477  testing with small sample size: Results and comparison, Atmos Pollut Res, 8(1), 154-163, doi:10.1016/j.apr.2016.08.007,
478  2017.

479  Donahue, N. M., Robinson, A. L., Huff Hartz, K. E., Sage, A. M., and Weitkamp, E. A.: Competitive oxidation in
480  atmospheric aerosols: The case for relative kinetics, Geophys. Res. Lett., 32(16), doi:10.1029/2005gl022893, 2005.

481  Fortenberry, C., Walker, M., Dang, A., Loka, A., Date, G., de Caryalho, K. C., Morrison, G., and Williams, B.: Analysis
482  of indoor particles and gases and their evolution with natural ventilation, Indoor Air, 29(5), 761-779, doi:10.1111/ina.12584,
483  2019.

484  Gross, S., Iannone, R., Xiao, S., and Bertram, A. K.: Reactive uptake studies of NO3 and N2O5 on alkenoic acid,
485  alkanoate, and polyalcohol substrates to probe nighttime aerosol chemistry, PCCP, 11(36), 7792-7803,
486  doi:10.1039/b904741g, 2009.

487  Hays, M. D., Geron, C. D., Linna, K. J., Smith, N. D., and Schauer, J. J.: Speciation of gas-phase and fine particle
488  emissions from burning of foliar fuels, Environmental Science & Technology, 36(11), 2281-2295, doi:10.1021/es0111683,
489  2002.

490  He, L. Y., Hu, M., Huang, X. F., Yu, B. D., Zhang, Y. H., and Liu, D. Q.: Measurement of emissions of fine particulate
491  organic matter from Chinese cooking, Atmos. Environ., 38(38), 6557-6564, doi:10.1016/j.atmosenv.2004.08.034, 2004.

492  Ho, K. F., Huang, R. J., Kawamura, K., Tachibana, E., Lee, S. C., Ho, S. S. H., Zhu, T., and Tian, L.: Dicarboxylic
493  acids, ketocarboxylic acids, alpha-dicarbonyls, fatty acids and benzoic acid in PM$_{2.5}$ aerosol collected during
494  CAREBeijing-2007: an effect of traffic restriction on air quality, Atmos Chem Phys, 15(6), 3111-3123, doi:10.5194/acp-
495  15-3111-2015, 2015.

496  Hou, X. M., Zhuang, G. S., Sun, Y., and An, Z. S.: Characteristics and sources of polycyclic aromatic hydrocarbons
497  and fatty acids in PM$_{2.5}$ aerosols in dust season in China, Atmos. Environ., 40(18), 3251-3262,
498  doi:10.1016/j.atmosenv.2006.02.003, 2006.

499  Huang, D. D., Zhu, S. H., An, J. Y., Wang, Q. Q., Qiao, L. P., Zhou, M., He, X., Ma, Y. G., Sun, Y. L., Huang, C., Yu,
500  J. Z., and Zhang, Q.: Comparative Assessment of Cooking Emission Contributions to Urban Organic Aerosol Using Online
501  Molecular Tracers and Aerosol Mass Spectrometry Measurements, Environmental Science & Technology, 55(21), 14526-
502  14535, doi:10.1021/acs.est.1c03280, 2021.

503  Huang, X. Q., Han, D. M., Cheng, J. P., Chen, X. J., Zhou, Y., Liao, H. X., Dong, W., and Yuan, C.: Characteristics

and health risk assessment of volatile organic compounds (VOCs) in restaurants in Shanghai, Environ Sci Pollut R, 27(1), 490-499, doi:10.1007/s11356-019-06881-6, 2020.

Kanakidou, M., Seinfeld, J. H., Pandis, S. N., Barnes, I., Dentener, F. J., Facchini, M. C., Van Dingenen, R., Ervens, B., Nenes, A., Nielsen, C. J., Swietlicki, E., Putaud, J. P., Balkanski, Y., Fuzzi, S., Horth, J., Moortgat, G. K., Winterhalter, R., Myhre, C. E. L., Tsigaridis, K., Vignati, E., Stephanou, E. G., and Wilson, J.: Organic aerosol and global climate modelling: a review, Atmos Chem Phys, 5, 1053-1123, doi:10.5194/acp-5-1053-2005, 2005.

Kawamura, K., Tachibana, E., Okuzawa, K., Aggarwal, S. G., Kanaya, Y., and Wang, Z. F.: High abundances of water-soluble dicarboxylic acids, ketocarboxylic acids and alpha-dicarbonyls in the mountaintop aerosols over the North China Plain during wheat burning season, Atmos Chem Phys, 13(16), 8285-8302, doi:10.5194/acp-13-8285-2013, 2013.

Lee, S., Liu, W., Wang, Y. H., Russell, A. G., and Edgerton, E. S.: Source apportionment of $PM_{2.5}$: Comparing PMF and CMB results for four ambient monitoriniz sites in the southeastern United States, Atmos. Environ., 42(18), 4126-4137, doi:10.1016/j.atmosenv.2008.01.025, 2008.

Li, L., Wu, D., Chang, X., Tang, Y., Hua, Y., Xu, Q. C., Deng, S. H., Wang, S. X., and Hao, J. M.: Polar organic aerosol tracers in two areas in Beijing-Tianjin-Hebei region: Concentration comparison before and in the sept. Third Parade and sources, Environ. Pollut., 270, doi:10.1016/j.envpol.2020.116108, 2021.

Li, R., Wang, Q. Q., He, X., Zhu, S. H., Zhang, K., Duan, Y. S., Fu, Q. Y., Qiao, L. P., Wang, Y. J., Huang, L., Li, L., and Yu, J. Z.: Source apportionment of $PM_{2.5}$ in Shanghai based on hourly organic molecular markers and other source tracers, Atmos Chem Phys, 20(20), 12047-12061, doi:10.5194/acp-20-12047-2020, 2020.

Makkonen, U., Virkkula, A., Mantykentta, J., Hakola, H., Keronen, P., Vakkari, V., and Aalto, P. P.: Semi-continuous gas and inorganic aerosol measurements at a Finnish urban site: comparisons with filters, nitrogen in aerosol and gas phases, and aerosol acidity, Atmos Chem Phys, 12(12), 5617-5631, doi:10.5194/acp-12-5617-2012, 2012.

Moise, T., and Rudich, Y.: Reactive uptake of ozone by aerosol-associated unsaturated fatty acids: Kinetics, mechanism, and products, J. Phys. Chem. A, 106(27), 6469-6476, doi:10.1021/jp025597e, 2002.

Nah, T., Kessler, S. H., Daumit, K. E., Kroll, J. H., Leone, S. R., and Wilson, K. R.: Influence of Molecular Structure and Chemical Functionality on the Heterogeneous OH-Initiated Oxidation of Unsaturated Organic Particles, J. Phys. Chem. A, 118(23), 4106-4119, doi:10.1021/jp502666g, 2014.

Nicolosi, E. M. G., Quincey, P., Font, A., and Fuller, G. W.: Light attenuation versus evolved carbon (AVEC) - A new way to look at elemental and organic carbon analysis, Atmos. Environ., 175, 145-153, doi:10.1016/j.atmosenv.2017.12.011, 2018.

Norris, G., Duvall, R., Brown, S., and Bai, S.: EPA Positive Matrix Factorization (PMF) 5.0 Fundamentals and User Guide, 2014.

Oliveira, C., Pio, C., Alves, C., Evtyugina, M., Santos, P., Goncalves, V., Nunes, T., Silvestre, A. J. D., Palmgren, F., Wahlin, P., and Harrad, S.: Seasonal distribution of polar organic compounds in the urban atmosphere of two large cities from the North and South of Europe, Atmos. Environ., 41(27), 5555-5570, doi:10.1016/j.atmosenv.2007.03.001, 2007.

Pei, B., Cui, H. Y., Liu, H., and Yan, N. Q.: Chemical characteristics of fine particulate matter emitted from commercial cooking, Front Env Sci Eng, 10(3), 559-568, doi:10.1007/s11783-016-0829-y, 2016.

Pleik, S., Spengler, B., Schafer, T., Urbach, D., Luhn, S., and Kirsch, D.: Fatty Acid Structure and Degradation Analysis in Fingerprint Residues, J. Am. Soc. Mass. Spectrom., 27(9), 1565-1574, doi:10.1007/s13361-016-1429-6, 2016.

Ren, H. X., Xue, M., An, Z. J., Zhou, W., and Jiang, J. K.: Quartz filter-based thermal desorption gas chromatography mass spectrometry for in-situ molecular level measurement of ambient organic aerosols, J. Chromatogr. A, 1589, 141-148, doi:10.1016/j.chroma.2019.01.010, 2019.

Ringuet, J., Leoz-Garziandia, E., Budzinski, H., Villenave, E., and Albinet, A.: Particle size distribution of nitrated

546 and oxygenated polycyclic aromatic hydrocarbons (NPAHs and OPAHs) on traffic and suburban sites of a European

547 megacity: Paris (France), Atmos Chem Phys, 12(18), 8877-8887, doi:10.5194/acp-12-8877-2012, 2012.

548     Rogge, W. F., Hildemann, L. M., Mazurek, M. A., Cass, G. R., and Simoneit, B.: Sources of fine organic aerosol. 4.

549 Particulate abrasion products from leaf surfaces of urban plants, Environmental Science & Technology, 27(13), 2700-2711,

550 1993.

551     Rogge, W. F., Medeiros, P. M., and Simoneit, B. R. T.: Organic marker compounds for surface soil and fugitive dust

552 from open lot dairies and cattle feedlots, Atmos. Environ., 40(1), 27-49, doi:10.1016/j.atmosenv.2005.07.076, 2006.

553     Schauer, C., Niessner, R., and Poschl, U.: Polycyclic aromatic hydrocarbons in urban air particulate matter: Decadal

554 and seasonal trends, chemical degradation, and sampling artifacts, Environmental Science & Technology, 37(13), 2861-

555 2868, doi:10.1021/es034059s, 2003.

556     Schauer, J. J., Kleeman, M. J., Cass, G. R., and Simoneit, B. R. T.: Measurement of emissions from air pollution

557 sources. 3. C-1-C-29 organic compounds from fireplace combustion of wood, Environmental Science & Technology, 35(9),

558 1716-1728, doi:10.1021/es001331e, 2001.

559     Schauer, J. J., Kleeman, M. J., Cass, G. R., and Simoneit, B. R. T.: Measurement of emissions from air pollution

560 sources. 4. C-1-C-27 organic compounds from cooking with seed oils, Environmental Science & Technology, 36(4), 567-

561 575, doi:10.1021/es002053m, 2002.

562     Simoneit, B. R. T.: Biomass burning - A review of organic tracers for smoke from incomplete combustion, Appl.

563 Geochem., 17(3), 129-162, doi:10.1016/S0883-2927(01)00061-0, 2002.

564     Thornberry, T., and Abbatt, J. P. D.: Heterogeneous reaction of ozone with liquid unsaturated fatty acids: detailed

565 kinetics and gas-phase product studies, PCCP, 6(1), 84-93, doi:10.1039/b310149e, 2004.

566     Tian, J. R., Qi, D. S., Wan, C., Liu, S. X., Wu, D. T., Qin, W., Dong, H. M., and Zhang, Q.: Quality assessment of

567 frying oil using short-chain fatty acid profile and infrared spectrum coupled with partial least squares, J Food Meas Charact,

568 14(4), 2289-2299, doi:10.1007/s11694-020-00476-3, 2020.

569     Vesna, O., Sax, M., Kalberer, M., Gaschen, A., and Ammann, M.: Product study of oleic acid ozonolysis as function

570 of humidity, Atmos. Environ., 43(24), 3662-3669, doi:10.1016/j.atmosenv.2009.04.047, 2009.

571     Wang, Q., Shao, M., Zhang, Y., Wei, Y., Hu, M., and Guo, S.: Source apportionment of fine organic aerosols in Beijing,

572 Atmos Chem Phys, 9(21), 8573-8585, doi:10.5194/acp-9-8573-2009, 2009.

573     Wang, Q. Q., He, X., Huang, X. H. H., Griffith, S. M., Feng, Y. M., Zhang, T., Zhang, Q. Y., Wu, D., and Yu, J. Z.:

574 Impact of Secondary Organic Aerosol Tracers on Tracer-Based Source Apportionment of Organic Carbon and PM2.5: A

575 Case Study in the Pearl River Delta, China, Acs Earth Space Chem, 1(9), 562-571,

576 doi:10.1021/acsearthspacechem.7b00088, 2017.

577     Wang, Q. Q., He, X., Zhou, M., Huang, D. D., Qiao, L. P., Zhu, S. H., Ma, Y. G., Wang, H. L., Li, L., Huang, C.,

578 Huang, X. H. H., Xu, W., Worsnop, D., Goldstein, A. H., Guo, H., and Yu, J. Z.: Hourly Measurements of Organic Molecular

579 Markers in Urban Shanghai, China: Primary Organic Aerosol Source Identification and Observation of Cooking Aerosol

580 Aging, Acs Earth Space Chem, 4(9), 1670-1685, doi:10.1021/acsearthspacechem.0c00205, 2020.

581     Wang, Q. Q., and Yu, J. Z.: Ambient Measurements of Heterogeneous Ozone Oxidation Rates of Oleic, Elaidic, and

582 Linoleic Acid Using a Relative Rate Constant Approach in an Urban Environment, Geophys. Res. Lett., 48(19),

583 doi:10.1029/2021GL095130, 2021.

584     Yee, L. D., Isaacman-VanWertz, G., Wernis, R. A., Meng, M., Rivera, V., Kreisberg, N. M., Hering, S. V., Bering, M.

585 S., Glasius, M., Upshur, M. A., Be, A. G., Thomson, R. J., Geiger, F. M., Offenberg, J. H., Lewandowski, M., Kourtchev,

586 I., Kalberer, M., de Sa, S., Martin, S. T., Alexander, M. L., Palm, B. B., Hu, W. W., Campuzano-Jost, P., Day, D. A., Jimenez,

587 J. L., Liu, Y. J., McKinney, K. A., Artaxo, P., Viegas, J., Manzi, A., Oliveira, M. B., de Souza, R., Machado, L. A. T., Longo,

588   K., and Goldstein, A. H.: Observations of sesquiterpenes and their oxidation products in central Amazonia during the wet

589   and dry seasons, Atmos Chem Phys, 18(14), 10433-10457, doi:10.5194/acp-18-10433-2018, 2018.

590      Zahardis, J., and Petrucci, G. A.: The oleic acid-ozone heterogeneous reaction system: products, kinetics, secondary

591   chemistry, and atmospheric implications of a model system - a review, Atmos Chem Phys, 7, 1237-1274, doi:10.5194/acp-

592   7-1237-2007, 2007.

593      Zhang, K., Yang, L. M., Li, Q., Li, R., Zhang, D. P., Xu, W., Feng, J. L., Wang, Q. Q., Wang, W., Huang, L., Yaluk, E.

594   A., Wang, Y. J., Yu, J. Z., and Li, L.: Hourly measurement of PM2.5-bound nonpolar organic compounds in Shanghai:

595   Characteristics, sources and health risk assessment, Sci. Total Environ., 789, doi:10.1016/j.scitotenv.2021.148070, 2021.

596      Zhang, N., Han, B., He, F., Xu, J., Zhao, R. J., Zhang, Y. J., and Bai, Z. P.: Chemical characteristic of PM2.5 emission

597   and inhalational carcinogenic risk of domestic Chinese cooking, Environ. Pollut., 227, 24-30,

598   doi:10.1016/j.envpol.2017.04.033, 2017a.

599      Zhang, Q., Ning, Z., Shen, Z. X., Li, G. L., Zhang, J. K., Lei, Y. L., Xu, H. M., Sun, J., Zhang, L. M., Westerdahl, D.,

600   Gali, N. K., and Gong, X. S.: Variations of aerosol size distribution, chemical composition and optical properties from

601   roadside to ambient environment: A case study in Hong Kong, China, Atmos. Environ., 166, 234-243,

602   doi:10.1016/j.atmosenv.2017.07.030, 2017b.

603      Zhang, Y. X., Schauer, J. J., Zhang, Y. H., Zeng, L. M., Wei, Y. J., Liu, Y., and Shao, M.: Characteristics of particulate

604   carbon emissions from real-world Chinese coal combustion, Environmental Science & Technology, 42(14), 5068-5073,

605   doi:10.1021/es7022576, 2008.

606      Zhang, Y. X., Shao, M., Zhang, Y. H., Zeng, L. M., He, L. Y., Zhu, B., Wei, Y. J., and Zhu, X. L.: Source profiles of

607   particulate organic matters emitted from cereal straw burnings, J Environ Sci, 19(2), 167-175, doi:10.1016/S1001-

608   0742(07)60027-8, 2007.

609      Zhao, X. Y., Hu, Q. H., Wang, X. M., Ding, X., He, Q. F., Zhang, Z., Shen, R. Q., Lu, S. J., Liu, T. Y., Fu, X. X., and

610   Chen, L. G.: Composition profiles of organic aerosols from Chinese residential cooking: case study in urban Guangzhou,

611   south China, J Atmos Chem, 72(1), 1-18, doi:10.1007/s10874-015-9298-0, 2015.

612      Zhao, Y. L., Hu, M., Slanina, S., and Zhang, Y. H.: Chemical compositions of fine particulate organic matter emitted

613   from Chinese cooking, Environmental Science & Technology, 41(1), 99-105, doi:10.1021/es0614518, 2007.

614      Ziemann, P. J.: Aerosol products, mechanisms, and kinetics of heterogeneous reactions of ozone with oleic acid in

615   pure and mixed particles, Faraday Discuss., 130, 469-490, 2005.

616